CrossMark

Influences of ^{7}Li enrichment on Th–U fuel breeding for an Improved Molten Salt Fast Reactor (IMSFR)

Guang-Chao Li[1,2,3] · Yang Zou[1,2,3] · Cheng-Gang Yu[1,2] · Jian-Long Han[1,2,3] · Jin-Gen Chen[1,2,3] · Hong-Jie Xu[1,2,3]

Abstract The molten salt fast reactor (MSFR) shows great promise with high breeding ratio (BR), large negative temperature coefficient of reactivity, high thermal–electric conversion efficiency, inherent safety, and online reprocessing. Based on an improved MSFR optimized by adding axial fertile salt and a graphite reflector, the influences of ^{7}Li enrichment on Th–U breeding are investigated, aiming to provide a feasible selection for the molten salt with high fissile breeding and a relatively low technology requirement for ^{7}Li concentration. With the self-developed molten salt reactor reprocessing sequence based on SCALE6.1, the burn-up calculations with online reprocessing are carried out. Parameters are explored including BR, ^{233}U production, double time (DT), spectrum, ^{6}Li inventory, neutron absorption, and the tritium production. The results show that the ^{7}Li enrichment of 99.95% is appropriate in the fast fission reactor. In this case, BR above 1.10 can be achieved for a long time, corresponding to the ^{233}U production of 130 kg per year and DT of 36 years. After 80 years' operation, the tritium production for 99.5% is only about 7 kg, and there is no obvious increase compared to that for 99.9995%.

Keywords IMSFR · ^{7}Li enrichment · Thorium · Fuel breeding

✉ Jin-Gen Chen
  chenjg@sinap.ac.cn

✉ Hong-Jie Xu
  xuhongjie@sinap.ac.cn

  Guang-Chao Li
  liguangchao@sinap.ac.cn

1 Shanghai Institute of Applied Physics, Chinese Academy of Sciences, Shanghai 201800, China

2 CAS Innovative Academies in TMSR Energy System, Shanghai 201800, China

3 University of Chinese Academy of Sciences, Beijing 100049, China

1 Introduction

Molten salt reactor (MSR), as the only liquid fuel reactor of the six candidate reactor types selected by the Generation-IV Forum (GIF), shows great promise with high thermal–electric conversion efficiency, inherent safety, as well as online reprocessing [1, 2]. Furthermore, the high breeding ratio (BR) and negative temperature coefficient of reactivity (TCR) have been demonstrated theoretically in the pure fission Molten Salt Fast Reactor (MSFR), and the long-life radioactive nuclides is of low production based on the Th–U fuel cycle [3, 4].

MSR originated from the Aircraft Reactor Experiment (ARE) [5], whose successful operating for 100 h in 1954 certified the feasibility of MSR for the first time. Then the Molten-Salt Reactor Experiment (MSRE) [6], using FLiBe salt as the fuel carrier, was developed by the Oak Ridge National Laboratory (ORNL) and ran 4.5 years from 1965, which proved the safety and reliability of MSR. Afterward, the Molten Salt Breeding Reactor (MSBR) [7] was proposed and studied by ORNL as well. The MSBR concept has an electrical power of 1 GWe, and the Th–U fuel

breeding can be achieved even in a thermal spectrum, providing that an efficient reprocessing of fission products (FPs) and Pa was involved. Unfortunately, this program was ended in 1976.

The MSBR concept was re-evaluated by the European Atomic Energy Community (Euratom). The results [8] show that the total TCR of MSBR is positive or slightly negative, and the complex reprocessing is a great challenge. Then, a no-graphite Molten Salt Fast Reactor (MSFR) [9, 10] was proposed by the French National Academy of Sciences (CNRS). This MSFR concept is attractive for the characters with a large negative TCR, no graphite lifetime limitation, low waste production, and high Th–U breeding ratio (BR). Researches [3, 11] on various fuels with different reprocessing efficiency in MSFR were carried out by Heuer et al. Findings include but are not limited to BR in equilibrium is 1.08 based on Th–U fuel cycle, and the corresponding production of ^{233}U is 95 kg per year, while the double time (DT) of ^{233}U is 56 years. The results also show that the reprocessing period declines from 4 m^3/day for MSBR to 40 L/day, because of the low neutron absorption cross section of FPs in fast spectrum.

Currently, the utilization of thorium with molten salt attracts lots of attention all over the world in both the fission and the fusion fields. For the pure fission reactors, besides the MSBR and MSFR, other reactors including AHTR in USA [12], FUJI series in Japan [13, 14], MOSART in Russia [15], also give the concept design with different targets. In 2011, the Strategic Project "Future Advanced Nuclear Energy–Thorium-based Molten Salt Reactor System (TMSR)" was launched by the Chinese Academy of Sciences (CAS), aiming to solve the key technical issues of TMSR and realizing the efficient utilization of Thorium [16]. For the fusion reactors, the molten salt blanket is used for high neutron wall loads and high efficient power conversion [17]. Researches show that the addition of fissile isotopes in the molten salt, such as Flibe + Weapon Grade (WG) PuF_4 or Spent Fuel Grade (SFG) PuF_4, could improve the neutronic performance and the energy multiplication in ARIES-ST [17]. In the improved fusion concept PACER, the molten salts of Flibe (92 mol%) mixed with ThF_4 and WG-PuF_4 were investigated [18]. The results show that tritium self-sufficiency is provided if the RG-PuF_4 is higher than 0.75 mol% and the ^{233}U production is about 2870 kg/year because of the existence of thorium in the molten salt and the large flux of neutrons with high energy produced by fusion. In the Laser Inertial Confinement Fusion–Fission Energy (LIFE) Engine, the neutronic performance is also investigated with the molten salt mixed with ^{233}U [19]. The results show that the tritium breeding ratio (TBR), the energy multiplication, and the fissile fuel breeding all increase with the increase of

^{233}U in the molten salt. The influences of ^{6}Li enrichment are studied as well, which indicates that the TBR increases while the fissile production decreases with the increase of the ^{6}Li enrichment.

Studies on the Th–U fuel cycle have been carried out in our group. They are mainly focused on the fission reactors, such as the analysis of Th–U fuel breeding in a graphite-moderated MSR [20] and in a ZrH-moderated MSR [21]. In the re-evaluation of MSFR, we found that the neutron absorption of alloy in the axial direction of the active core is so high that a considerable number of neutrons are wasted, and the utilization efficiency of the fertile salt is somewhat too low. So the geometry of MSFR was improved by adding fertile salt on the axis direction of the active core to improve the Th–U fuel breeding and by adding a graphite reflector for fertile saving [22]. Another problem is that the enrichment of ^{7}Li used in the molten salt of MSFR is 99.995%, which brings a great challenge to the purification technology. Even if it could be realized based on the present technology, the economic cost is too high.

In this paper, the influences of ^{7}Li enrichment are analyzed based on the pure fission improved MSFR (IMSFR), aiming to give an appropriate reference both suitable for high BR and low technological requirement. Section 2 gives the general description of IMSFR and the calculation tools. Then, the results of the burn-up calculations with online reprocessing are presented in Sect. 3. The influences of ^{7}Li enrichment are discussed from the aspects of BR, ^{233}U production and DT, spectrum, ^{6}Li inventory, and neutron absorption, as well as tritium production. Finally, the conclusion is given in Sect. 4.

2 General description of IMSFR and calculation tools

2.1 General description of IMSFR

The standard model of IMSFR is a pure fission fast reactor with a thermal power of 3000 MWth and a mean fuel temperature of 1023 K, which takes reference to the MSFR [3]. The cross and vertical sections of IMSFR are shown in Fig. 1, following with the main parameters in Table 1. There are mainly two partitions in the IMSFR, namely the fuel zone and the fertile zone, corresponding to the fuel salt and the fertile salt. The composition of the fuel salt is set as 22.5(HM)F_4–77.5LiF in mol%. For the Th–U fuel cycle, HM stands for the heavy metal initially composed of ^{232}Th and ^{233}U, and the ratio of ^{232}Th and ^{233}U is adjusted for the reactor criticality. The composition of the fertile salt is also 22.5(HM)F_4–77.5LiF in mol%, where the
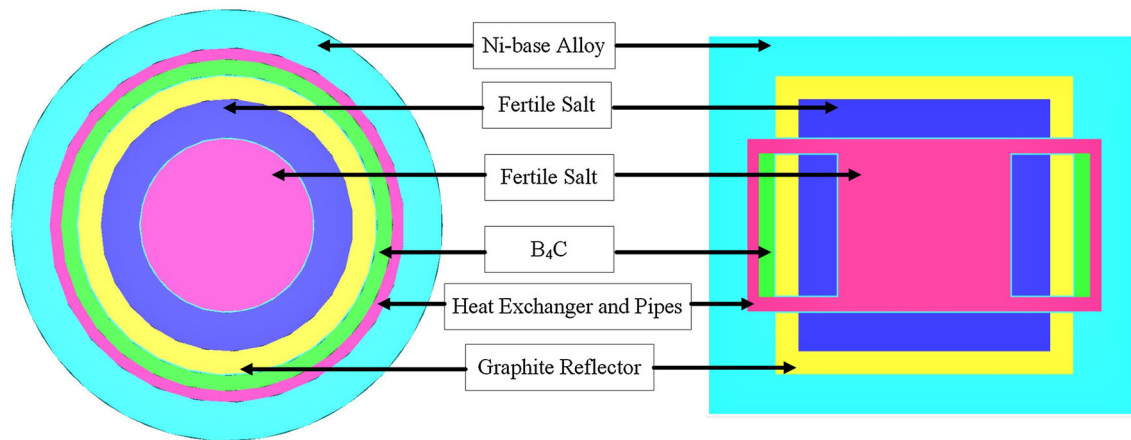
Fig. 1 (Color online) Cross and vertical sections of IMSFR

Table 1 Main parameters of the IMSFR

Parameters	Values
Thermal power (MWth)	3000
Composition of fuel salt (mol%)	77.5LiF–20ThF$_4$–2.5^{233}UF$_4$
Composition of fertile salt (mol%)	77.5LiF–22.5ThF$_4$
Temperature of fuel salt (K)	1023
Temperature of fertile salt (K)	973
Volume of fuel salt (m^3)	18
Volume of fertile salt (m^3)	8.45
Initial inventory of ^{233}U (t)	4.80
Initial inventory of ^{232}Th (t)	58.70 (fuel: 38.27 + fertile: 20.43)
Density of molten salt at 1023 K(g cm^{-3})	4.10
Dilatation coefficient (g cm^{-3} K^{-1})	-8.82×10^{-4}
Density of graphite (g cm^{-3})	2.30
Density of alloy (g cm^{-3})	8.86
Density of B$_4$C (g cm^{-3})	2.52
Enrichment of ^{10}B (%)	18.4
Diameter of the core (cm)	225.5
Height of the core (cm)	225.5
Reprocessing period of gas and insoluble heavy metal (s)	30
Reprocessing period of fuel salt (days)	450
Reprocessing period of fertile salt (days)	210

initial HM is only ^{232}Th. The proportion of (HM)F$_4$ is fixed at 22.5 mol% because of the low eutectic point of 838 K. The adopted enrichment of ^{7}Li in the MSFR is 99.995%, which will be further studied in this paper.

The fuel zone (red area shown in Fig. 1) consists of the active core and the external fuel circuit (including collectors, salt-bubble separators, heat exchangers, pumps, and pipes). The active core is a compact cylinder (height/diameter = 1) with a diameter of 225.5 cm. The liquid fuel salt flows through the core from the bottom to the top and then to the heat exchangers with 16 groups of pumps outside. At the same time, the heat produced by fission is taken out of the active core to the heat exchangers then to the secondary loop. The total volume of the fuel salt is 18 m^3, half of which is in the active core and the other half in the external circuit. The fertile salt surrounds the active core in both the radius direction and the axial direction with a thickness of 30 cm (blue area shown in Fig. 1). The fuel salt and the fertile salt are separated by the Ni-based alloy with a thickness of 2 cm. The activation products of the alloy have been studied in a fluoride salt-cooled high-temperature reactor (FHR) [23], but further study is still needed in the IMSFR to confirm its stability and security. Surrounding the fertile salt is the graphite reflector (yellow

area in Fig. 1), which is adopted to the fertile saving [22]. Between the external circuit of the fuel salt and the graphite reflector, B_4C of 10 cm (green area in Fig. 1) is arranged to stop the neutrons leaking out of the reactor. The most external surface is also Ni-based alloy which serves as the structure material. Continuous boundary conditions are adopted between the material of the fuel salt, the alloy, the fertile salt, graphite, and B_4C, while vacuum boundary condition is used outside the most layer out of the alloy.

2.2 Calculation tools: SCALE6.1 and MSR-RS

SCALE6.1 [24] is a comprehensive code package developed and maintained by ORNL, which can be used for criticality safety, burn-up calculation, radiation shielding, radioactive source term analysis, sensitivity and uncertainty analysis, and so on. In this paper, the module of CSAS (Criticality Safety Analysis) is used for the criticality calculation, the TRITON (Transport Rigor Implemented with Time-dependent Operation for Neutronic depletion) module performs for the problem-dependent cross-section processing and multi-group neutron transport calculation, and the ORIGEN-S (Oak Ridge Isotope Generation Code System) module serves for the depletion and decay calculations. The KMART6 (Keno Module for Activity-Reaction Rate Tabulation) module is used for the reaction rate of relevant nuclides. Other modules are also invoked, such as CENTRM/PMC and BONAMI which process the cross sections in the resolved and unresolved resonance energy regions, respectively.

For MSR, the online reprocessing is an outstanding feature compared to the traditional solid fuel reactors. The extraction of FPs brings great advantages on the neutron economy and the Th–U fuel breeding. In addition, ^{233}U and ^{232}Th can be refueled on line for the reactor criticality, which is beneficial to decrease the excess reactivity and the inventory of fissile. However, tools at hand, such as MCNPX and SCALE, are not sufficient to simulate the complex reprocessing, especially for the functions of refueling and extracting with changing rates versus time. So the module of MSR-RS based on SCALE6.1 was developed particularly for the burn-up simulation of MSR in our previous work [25, 26].

The flowchart of MSR-RS is shown in Fig. 2. First, the geometry and the molten salts are initialized for the input files. Second, the neutron transportation and depletion are calculated by TRITON and ORIGEN-S. Meanwhile, FPs are removed and ^{233}Pa is extracted as well to decay into ^{233}U out of the core. In addition, ^{233}U and ^{232}Th are injected into the fuel salt in order to maintain the reactor criticality and keep the inventory of HN constant. The
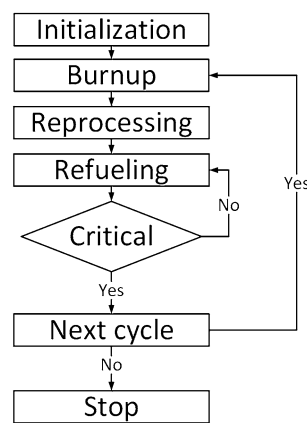
Fig. 2 Flowchart of MSR-RS

cycle calculation is performed iteratively until the depletion time reaches the value set by the user. A 238-group cross-section database is selected in this paper, and 388 nuclides are tracked in the trace quantities.

In every step of the depletion calculations, about 1600 nuclides are tracked including fissions and decays. For the nuclide i, the burn-up equation is shown in Eq. (1):

$$\frac{dN_i}{dt} = \sum_{j=1}^{m} l_{ij}\lambda_j N_j + \bar{\phi}\sum_{j=1}^{m} f_{ij}\sigma_j N_j - (\lambda_i + \bar{\phi}\sigma_i)N_i \\ - \lambda_i^r N_i + B_i \quad i = (1, 2, \ldots, m),$$

(1)

in which N_i is the atom density of nuclide i, λ_i is the decay constant, σ_i is the one group absorption cross section, $\bar{\phi}$ is the average neutron flux, l_{ij} is the branch ratio to i when j decays, and f_{ij} is the branch ratio to i after j absorbs a nuetron. The last two parameters $\lambda_i^r N_i$ and B_i stand for the rates of extracting and refueling , respectively. And $\lambda_i^r = \epsilon/T_r$ is the parameter similar to the decay constant. ϵ stands for the efficiency of reprocessing, and T_r is the period of reprocessing. In this paper, the extraction of FPs and the refueling of ^{233}U and ^{232}Th are realized by changing these reprocessing parameters in ORIGEN-S.

The online reprocessing includes the refueling of HN and the extracting of FPs. The extracting system involves two key processes [3]. One is the mechanical extraction of gaseous FPs and non-dissolved metals via an online He gas bubbling system. The other is the chemical removal of lanthanides and other soluble FPs via batch reprocessing by the on-site facilities. The He gas bubbling system can remove the gaseous FPs and the non-dissolved metals rapidly, so the remove period is set as 30 s. The chemical reprocessing is relatively slow and is set as 40 L/day. The fuel salt and the fertile salt are $18\,m^3$ and $8.45\,m^3$, respectively, so their reprocessing periods are 450 and 210 days. Meanwhile, ^{233}Pa and ^{233}U in the fertile salt are also extracted along with the molten salt reprocessing, aiming

to reduce its neutron absorption and improve the Th–U conversion capability. Because of the online refueling which makes it possible for MSR with low excess reactivity, the effective multiplication factor ($Keff$) is set at 1.005 ± 0.005 during all the operating time.

3 Results and discussions

Burn-up calculations are carried out with MSR-RS based on the IMSFR, and the influences of ^{7}Li enrichment from 98 to 99.9995% are explored. The BR, DT, and ^{233}U production are demonstrated in Sects. 3.1 and 3.2, and reasons are explored from the aspects of spectrum, ^{6}Li inventory, and neutron absorption in Sects. 3.3 and 3.4. Finally, the tritium production is analyzed in Sect. 3.5.

3.1 Th–U breeding ratio

BR is defined by the product rate over the disappearance rate of fissile, or the capture rate of fertile over the absorption rate of fissile. For Th–U fuel cycle, it can be expressed as [20]:

$$\mathrm{BR} = \frac{R_c^{232\mathrm{Th}} + R_c^{234\mathrm{U}} - R_c^{233\mathrm{Pa}}}{R_a^{233\mathrm{U}} + R_a^{235\mathrm{U}}}, \tag{2}$$

in which $R\,a$ and $R\,c$ stand for the neutron capture rate and the absorption rate, respectively.

The results are shown in Fig. 3. From the chart we can see that, when the enrichment of ^{7}Li is 99.995%, BR is approximately at 1.11 in equilibrium based on the improved geometry. It is obviously promoted when compared to that in the reference MSFR [3], which results from the contribution of the fertile salt in the axial direction.

As also can be seen from the chart, when the enrichment is above 99.95%, BR's evolution with time keeps nearly the same. But when the enrichment is 98%, BR declines drastically to less than 1.0 because of the neutron
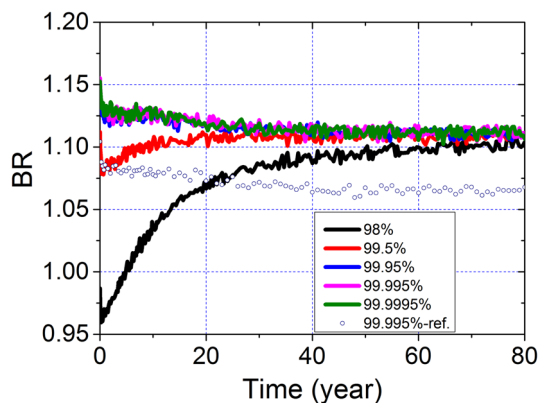
Fig. 3 (Color online) BR's evolution versus the enrichment of ^{7}Li

absorption of ^{6}Li. Then, ^{6}Li is consumed (more detailed discussion is shown in Sect. 3.4) and its neutron absorption decreases as the evolution of the reactor, leads to an increase of BR. After about 50 years' evolution, BR, with different enrichments of ^{7}Li, tend to be the same. We also notice that BR declines rapidly at the early time, and it is because of the accumulation of FPs. In short, according to the evolution of BR, the enrichment of ^{7}Li could be set at the range between 99.5 and 99.95% rather than 99.995%.

3.2 ^{233}U production and double time

When BR is bigger than 1.0, the fissile produced is more than that consumed. For the IMSFR with online reprocessing, the extracted ^{233}Pa from the fertile salt decays to ^{233}U in half a year. The ^{233}U extracted from the core and that decayed from ^{233}Pa are partially refueled into the active core for criticality, and the remaining (if any is left) is the net ^{233}U production, which is defined as:

$$M = M_{ex}^{233\mathrm{U}} + M_{ex}^{233\mathrm{Pa}} - M_{re}^{233\mathrm{U}}, \tag{3}$$

where ex and re stand for extracting and refueling, respectively. For more clarity, the relative ^{233}U production (M_r) is used in this paper. It is obtained by dividing the net ^{233}U production to the initial inventory of ^{233}U (M_0), which is expressed as:

$$M_r = \frac{M_{ex}^{233\mathrm{U}} + M_{ex}^{233\mathrm{Pa}} - M_{re}^{233\mathrm{U}}}{M_0}. \tag{4}$$

That is to say, when M_r reaches 1.0, the net production of ^{233}U equals that of M_0 (4.8 t), which means the fissile doubles and it is sufficient to start a new IMSFR. The corresponding time is DT. Hence, the ^{233}U production per year can be derived as the following equation:

$$m = M_0/DT. \tag{5}$$

Figure 4 presents M_r versus time, while Fig. 5 exhibits DT and the ^{233}U production per year with the different ^{7}Li enrichment. As shown in the two figures, when the enrichment of ^{7}Li is 99.995%, the production rate of ^{233}U promotes from 95 kg/year in the reference MSFR [3] to 130 kg/year in the IMSFR, while DT shortens from 56 years to 36 years. The advantages of the IMSFR are certified again from the aspects of ^{233}U production and DT.

As also shown from Fig. 4, when the enrichment is above 99.95%, the ^{233}U production in different cases is nearly the same. There is no obvious improvement on Th–U fuel breeding when the enrichment is 99.9995% compared to that for 99.95%, and this is the same with DT and the ^{233}U production rate as show in Fig. 5. When the enrichment is 99.5%, the ^{233}U production declines and the
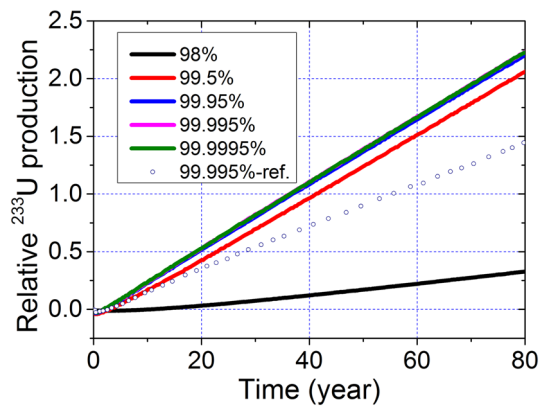
Fig. 4 (Color online) Relative ^{233}U production versus the enrichment of ^{7}Li
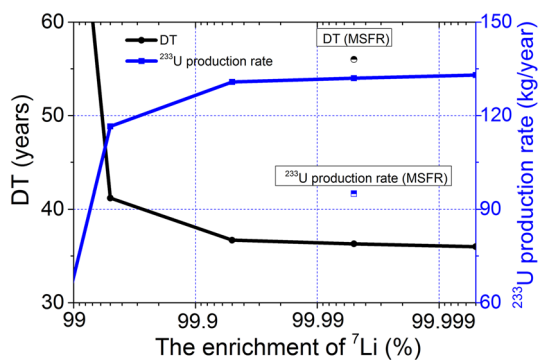
Fig. 5 (Color online) DT and ^{233}U production rate versus the enrichment of ^{7}Li

DT extends to more than 40 years. For the case of 98%, the net ^{233}U production even could not reach the initial inventory in 80 years. In short, taking into account the ^{233}U production and DT, the ^{7}Li enrichment should be set at the range between 99.5 and 99.95%. 99.95% is recommended in the IMSFR because it is suitable for both Th–U fuel breeding and a relatively low technical requirement on ^{7}Li purification.

3.3 Spectrum

In this section, the normalized lethargy spectral are explored to understand the influences of ^{7}Li enrichment on Th–U fuel breeding more deeply.

Figure 6a, b gives the spectra at the initial time with a series of ^{7}Li enrichment for the fuel salt and fertile salt, respectively. As shown in Fig. 6a, there is no obvious distinction in the fuel salt with different ^{7}Li enrichment. However, when it comes to the fertile salt, significant differences appear, as shown in Fig. 6b. The lower the ^{7}Li enrichment is, the harder the spectrum is. The reason is that the neutrons generated in the active core are moderated

during the traveling from the fuel salt to the fertile salt, and the neutron absorption cross section of ^{6}Li is much bigger in the low-energy region than in the high-energy region. Therefore, when there is plenty of ^{6}Li in the fertile salt, the low-energy neutrons are absorbed, leading to the decline of the spectrum in the low-energy region. The little deviation of spectra in the fuel salt is also because of the absorption of ^{6}Li. When the ^{7}Li enrichment is higher than 99.95%, there is not enough ^{6}Li, so the spectrum keeps nearly the same as the case of 99.9995%. In other words, the ^{7}Li enrichment of 99.95% is recommended as well from the aspect of spectrum.

Then, in the second part of this section, the spectral's evolution with time is studied in the case that the ^{7}Li enrichment is 99.95%. The results are exhibited in Fig. 6c, d, which are also corresponding to the fuel salt and the fertile salt. From the chart we can see that the spectra in both the fuel salt and the fertile salt have almost no change from the startup to the 60th year. Only a little deviation appears which mainly results from the large neutron absorption cross section of FPs, such as Xe and Sm.

In a word, the enrichment of ^{7}Li has a more important influence on spectrum in the fertile salt than that in the fuel salt, which is because the neutron absorption cross section of ^{6}Li in the low-energy region is larger than that in the high-energy region.

3.4 Inventory of ^{6}Li and neutron absorption

Further researches are carried out by analyzing the inventory of ^{6}Li and the neutron absorption of the main nuclides, including ^{6}Li, ^{232}Th, and ^{233}U. Figure 7 gives the evolution of ^{6}Li with different enrichments of ^{7}Li. As can be seen from the chart, when the enrichment of ^{7}Li is higher than 99.95%, the inventory of ^{6}Li in the core is less than 5 g, which is so little that it has almost no effect on the thermal neutrons. However, when the enrichment of ^{7}Li is 99.5% or less, the mass of ^{6}Li is more than 20 g, which significantly affects the neutron absorption as well as the Th–U fuel breeding.

The relative neutron absorption of the main nuclides versus the enrichment of ^{7}Li is given in Fig. 8 at the startup time and at the 36th year (DT is 36 years when the enrichment of ^{7}Li is 99.95%). The solid line stands for the neutron absorption at startup. Information can be obtained from the chart that the neutron absorption of ^{6}Li declines as the increasing of the ^{7}Li enrichment due to the decline of ^{6}Li's inventory. Meanwhile, the absorption of ^{232}Th increases while the absorption of ^{233}U keeps nearly the same. So according to Eq. (2), BR increases and then tends to equilibrium with the increasing of ^{7}Li enrichment. That
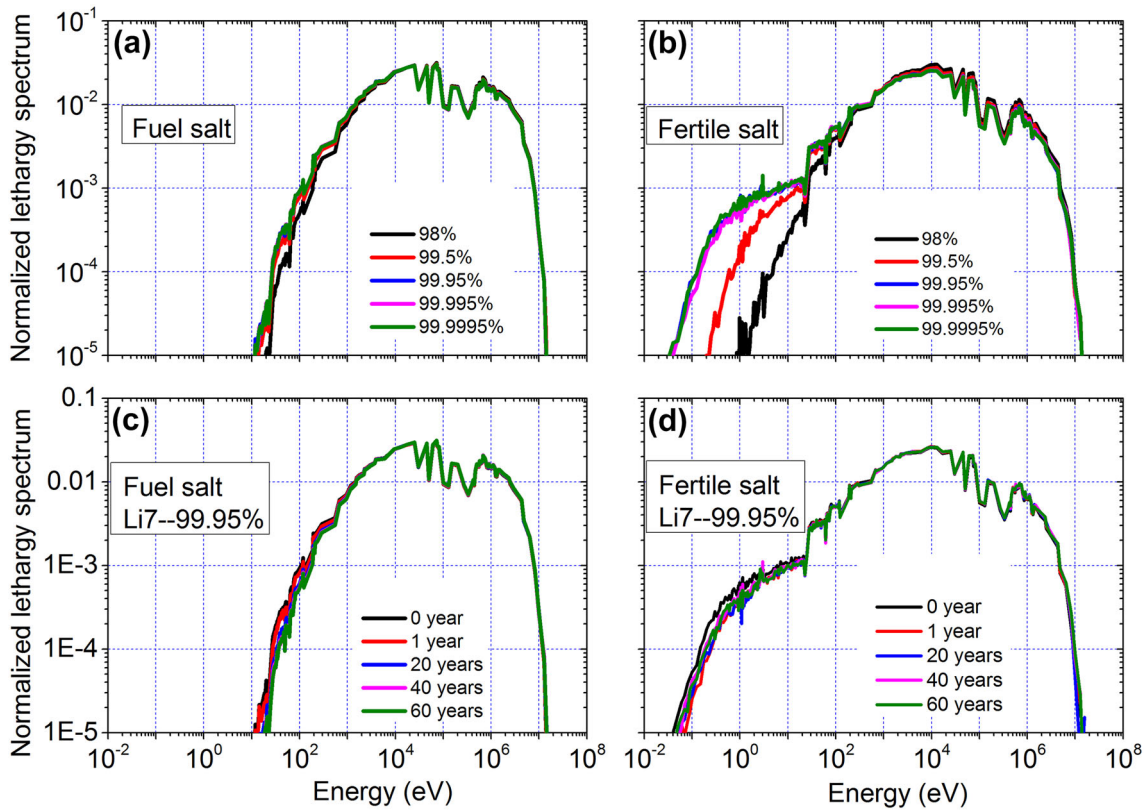
Fig. 6 (Color online) Normalized lethargy spectrum of fuel salt and fertile salt at initial time with different ^{7}Li enrichment (**a**, **b**) and spectral evolution with time when the enrichment is 99.5% (**c**, **d**)
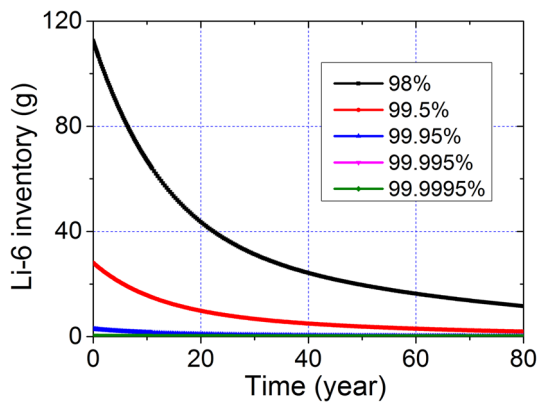
Fig. 7 (Color online) Inventory of ^{6}Li versus time with different enrichment of ^{7}Li

Fig. 8 (Color online) Relative neutron absorption versus the enrichment of ^{7}Li at startup and at the 36th year

is to say, when the enrichment of ^{7}Li is 99.5% or lower, the neutron absorption of ^{6}Li is so high that a certain number of neutrons are wasted, which leads to the reduction of ^{232}Th's neutron capture. When the enrichment is higher than 99.95%, the neutron absorption of ^{6}Li is relatively low, and it has little influence on ^{232}Th's neutron capture. The dashed line in Fig. 8 represents the absorption at the 36th year. As shown in the chart, the neutron absorption of ^{6}Li, ^{232}Th, and ^{233}U change a little with the variation of the

^{7}Li enrichment. That is because after 36 years' burn-up, ^{6}Li is consumed to a very low level, which has been shown in Fig. 7.

Then, the neutron absorption at startup and at the 36th year are compared in Fig. 8. When the enrichment of ^{7}Li is 99.95%, the neutron absorption of ^{232}Th and ^{233}U is slightly lower at the 36th year than that at startup. That's because of the accumulation of FPs, which absorbs a

certain amount of neutrons in the core. Fortunately, with the online reprocessing, the influence of FPs has decreased to a very low level.

3.5 Tritium production

In the MSRE, it is found that the tritium is mainly from the irradiation of ^{6}Li [27], and the generation reaction is as follows:

$$n +^6 \mathrm{Li} \rightarrow^3 \mathrm{H} +^4 \mathrm{He}. \tag{6}$$

In the IMSFR with LiF molten salt, the decrease of ^{7}Li enrichment would inevitably lead to the increase of ^{6}Li inventory and the production of tritium. For the fusion reators, the production of tritium is useful to the D–T fusion reaction, so the increase of ^{6}Li in the Flibe or LiF molten salt contributes to the TBR and the tritium self-sufficiency [19]. However, the IMSFR concept is a pure fission fast reactor but not a fusion one. The tritium is extracted as the He gas bubbling because it is undissolved in the molten salt, and following work is needed to collect it. So it is undesired for the possibility of releasing to the atmosphere [28] and should be as little as possible in the fission reactor. In this subsection, the production of tritium is investigated finally.

As shown in Fig. 9, after 80 years' operation, the tritium production is about 7 kg when the enrichment of ^{7}Li is 99.95%, and it is nearly the same to the case of 99.9995%. But when the enrichment of ^{7}Li is 99.5%, the production of tritium is more than 11 kg. And it even reaches to nearly 30 kg in the 80th year when the enrichment of ^{7}Li is 98%. So when the ^{7}Li enrichment of 99.5% is still recommended from the aspect of tritium production.
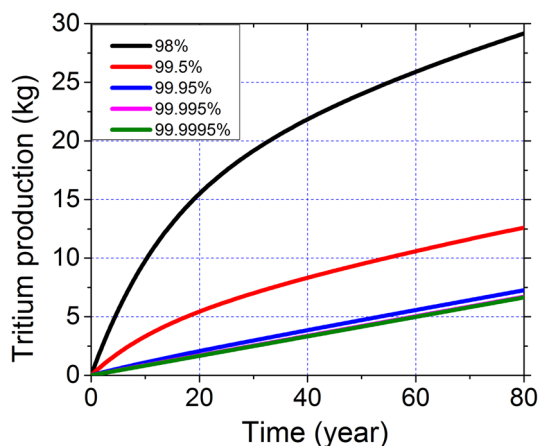
Fig. 9 (Color online) Tritium production with different enrichment of ^{7}Li

4 Conclusion

In this paper, the influences of ^{7}Li enrichment on BR, ^{233}U production, DT, spectrum, ^{6}Li inventory, neutron absorption, and tritium production are analyzed by MSR-RS based on the IMSFR. Conclusion can be reached that:

- There is no obvious improvement on Th–U fuel breeding when the enrichment of ^{7}Li is 99.9995% compared to that for 99.95% in the molten salt fast reactor. There is also no obvious increase on the tritium production when the ^{7}Li enrichment is 99.95% compared to that for 99.9995%.
- When the enrichment of ^{7}Li is lower than 99.5%, the Th–U breeding is influenced obviously, mainly because of the high neutron absorption of ^{6}Li, which leads to the decline of ^{232}Th's neutron capture.
- The ^{7}Li enrichment of 99.95% is appreciated and recommended for the IMSFR. Burn-up calculations show that when the enrichment is 99.95%, BR is about 1.11 in equilibrium is achieved and the net ^{233}U production is 130 kg per year, corresponding to a DT of 36 years and the tritium production of about 7 kg after 80 years' operation.

References

1. U.S. DOE, A technology roadmap for generation IV nuclear energy system. Philos. Rev. **66**, 239–241 (2002)
2. J. Serp, M. Allibert, O. Beneš et al., The molten salt reactor (MSR) in generation IV: overview and perspectives. Prog. Nucl. Energy **77**, 308–319 (2014). doi:10.1016/j.pnucene.2014.02.014
3. D. Heuer, E. Merle-Lucotte, M. Allibert et al., Towards the thorium fuel cycle with molten salt fast reactors. Ann. Nucl. Energy **64**, 421–429 (2014). doi:10.1016/j.anucene.2013.08.002
4. Nuclear Fuel Cycle and Materials Section, Thorium fuel cycle-potential benefits and challenges (IAEA-TECDOC-1450). Vienna: IAEA, vol. 48, pp. 1–3 (2005)
5. E.S. Bettis, R.W. Schroeder, G.A. Cristy et al., The aircraft reactor experiment-design and construction. Nucl. Sci. Eng. **2**, 804–825 (1957)
6. P.N. Haubenreich, J.R. Engel, Experience with the molten-salt reactor experiment. Nucl. Appl. Technol. **8**, 118–136 (1967)
7. R.C. Robertson, Conceptual design study of a single-fluid molten-salt breeder reactor. Boilers **ORNL–4541**, 1–200 (1970)
8. A. Nuttin, D. Heuer, A. Billebaud et al., Potential of thorium molten salt reactors: detailed calculations and concept evolution with a view to large scale energy production. Prog. Nucl. Energy **46**, 77–99 (2005). doi:10.1016/j.pnucene.2004.11.001
9. L. Mathieu, D. Heuer, R. Brissot et al., The thorium molten salt reactor: moving on from the MSBR. Prog. Nucl. Energy **48**, 664–679 (2006). doi:10.1016/j.pnucene.2006.07.005
10. L. Mathieu, D. Heuer, E. Merle-Lucotte et al., Possible config-urations for the thorium molten salt reactor and advantages of the fast nonmoderated version. Nucl. Sci. Eng. **161**, 78–89 (2009)

11. E. Merle-Lucotte, D. Heuer, M. Allibert, et al., Minimizing the fissile inventory of the molten salt fast reactor. Advances in Nuclear Fuel Management IV (ANFM IV), Hilton Head Island, USA (2009)

12. C.W. Forsberg, P.F. Peterson, R.A. Kochendarfer, in *Design options for the advanced high-temperature reactor*. Proceedings of ICAPP 2008 (Anaheim, 2008), pp. 8026

13. K. Mitachi, T. Yamamoto, R. Yoshioka, Three-region core design for 200-MW (electric) molten-salt reactor with thorium–uranium fuel. Nucl. Technol. **158**, 348–357 (2007)

14. M. Koshi, Y. Takahisa, R. Yoshioka, Self-sustaining core design for 200 MWe molten-salt reactor with thorium–uranium fuel: Fuji-u3-(0). International Workshop on Thorium Utilization for Sustainable Development of Nuclear Energy, Tsinghua University (2007)

15. V. Ignatiev, O. Feynberg, I. Gnidoi et al., Molten salt actinide recycler and transforming system without and with Th–U support: fuel cycle flexibility and key material properties. Ann. Nucl. Energy **64**, 408–420 (2014). doi:10.1016/j.anucene.2013.09.004

16. M.H. Jiang, H.J. Xu, Z.M. Dai, Advanced fission energy program-TMSR nuclear energy system. Bull. Chin. Acad. Sci. **27**, 366–374 (2012) **(in Chinese)**

17. Ü. Mustafa, A. Acır, Neutronic investigation on the ARIES-ST fusion reactor with fissionable molten salts. Energy Convers. Manag. **51**, 2531–2534 (2010). doi:10.1016/j.enconman.2010.05.018

18. A. Acır, Improvement of the neutronic performance of the PACER fusion concept using thorium molten salt with reactor grade plutonium. J. Fusion Energy **32**, 11–14 (2013). doi:10.1007/s10894-012-9518-4

19. A. Acır, Neutronic analysis of the laser inertial confinement fusion-fission energy (LIFE) engine using various thorium molten salts. J. Fusion Energy **32**, 634–641 (2013). doi:10.1007/s10894-013-9628-7

20. C.Y. Zou, X.Z. Cai, D.Z. Jiang et al., Optimization of temperature coefficient and breeding ratio for a graphite-moderated molten salt reactor. Nucl. Eng. Des. **281**, 114–120 (2015). doi:10.1016/j.nucengdes.2014.11.022

21. P. Wu, X.Z. Cai, C.G. Yu et al., Preliminary analysis of Th–U conversion performance in a ZrH-moderated molten salt reactor. Nucl. Tech. **39**, 050605–050605 (2016). doi:10.11889/j.0253-3219.2016.hjs.39.050605 **(in Chinese)**

22. G.C. Li, Y. Zou, C.G. Yu et al., Model optimization and analysis of Th–U breeding based on MSFR. Nucl. Tech. **40**, 020603–020603 (2017). doi:10.11889/j.0253-3219.2017.hjs.40.020603 **(in Chinese)**

23. C. Peng, X.W. Zhu, G.Q. Zhang et al., Numerical analysis of the activity of irradiated alloy-N in an FHR. Nucl. Sci. Tech. **27**, 44–44 (2016). doi:10.1007/s41365-016-0044-3

24. ORNL, SCALE: a modular code system for performing standardized computer analyses for licensing evaluations. ORNL/TM-2005/39, Version 6.1 (2009)

25. C.G. Yu, X.X. Li, X.Z. Cai et al., Analysis of minor actinides transmutation for a Molten Salt Fast Reactor. Ann. Nucl. Energy **85**, 597–604 (2015). doi:10.1016/j.anucene.2015.06.014

26. C.G. Yu, X.X. Li, X.Z. Cai et al., Minor actinide incineration and Th–U breeding in a small FLiNaK Molten Salt Fast Reactor. Ann. Nucl. Energy **99**, 335–344 (2017). doi:10.1016/j.anucene.2010.09.024

27. G.T. Mays, A.N. Smith, J.R. Engel, Distribution and behavior of tritium in the coolant-salt technology facility. ORNL/TM-5759, pp. 1–69 (1977)

28. X.W. Zhu, Z.Z. He, C. Peng, et al., The analysis of tritium generation in the solid fuel thorium molten salt reactor in transactions of the American Nuclear Society. Washington (2013)